

## Experimental and Theoretical Investigation for Inhibition Action and Adsorption Behavior of Montelukast Sodium in 1 M HCl Solution

Priyanka Singh<sup>1</sup>, Ambrish Singh<sup>1</sup>, M.A. Quraishi<sup>1,\*</sup>, Eno E. Ebenso<sup>2</sup>

<sup>1</sup> Department of Applied Chemistry, Institute of Technology, Banaras Hindu University, Varanasi-221005

<sup>2</sup> Department of Chemistry, School of Mathematical & Physical Sciences, North-West University(Mafikeng Campus), Private Bag X2046, Mmabatho 2735, South Africa

\*E-mail: [maquraishi@rediffmail.com](mailto:maquraishi@rediffmail.com), [maquraishi.apc@itbhu.ac.in](mailto:maquraishi.apc@itbhu.ac.in)

Received: 7 July 2012 / Accepted: 9 August 2012 / Published: 1 September 2012

---

Inhibition behavior of Montelukast sodium (2-[1-[[1-[3-[2-[(7-Chloro-2-quinolyl)] vinyl] phenyl]-3-[2-(1-hydroxy-1-methyl-ethyl)phenyl]-propyl]sulfanylmethyl]cyclopropyl]acetic acid sodium salt) for corrosion of mild steel (MS) in 1 M HCl solution was studied by weight loss, electrochemical and quantum chemical methods. Montelukast sodium showed good inhibition efficiency (97% observed at 100 ppm). Polarization study indicated mixed-type nature of the inhibitor. The adsorption of the inhibitor followed Langmuir adsorption isotherm. Quantum chemical calculations provided good support for the adsorption of inhibitor molecules on the mild steel surface. Mechanism of inhibition was further corroborated by the values of activation parameters obtained from the experimental data. Optical microscopy was used to characterize the metal surface before and after adsorption of inhibitor.

---

**Keywords:** Montelukast sodium, Electrochemical measurements, Adsorption Isotherm, Quantum chemical measurements, Optical microscopy.

### 1. INTRODUCTION

Mild steel is used as constructional material in many industries because of its excellent mechanical properties and low cost [1]. Chemical industries frequently use concentrated acids for the removal of scale and rust from iron and steel. To prevent corrosion of metal use of inhibitors is a good option [2,3]. Organic compounds are mostly used in industry (for preventing corrosion) which mainly contains oxygen, sulphur, nitrogen atoms, and multiple bonds in the molecule through which they are adsorbed on metal surface [4]. Depending on the type of forces, adsorption can be physisorption,

chemisorption or a combination of both [5]. The replacement of harmful inhibitors with effective non-hazardous alternatives is due to the toxicity of widely used corrosion inhibitors and the ever tightening environmental regulations [6]. The extensive research and development in this area has resulted in the discovery of new classes of corrosion inhibitors, and emphasis on the use of several drugs such as Ziprasidone, Cefatrexyl, Ketoconazole, Ciprofloxacin, Norfloxacin, Ofloxacin, Sulfaguanidine, Sulfamethazine, Sulfamethoxazole, Sulfadiazine, Rhodanine azosulpha [7-12]. Drugs act as efficient corrosion inhibitors due to presence of  $\pi$  electrons, hetero atoms in their molecules through which they are either adsorbed or form insoluble metal complex at the metal surface and inhibit metal corrosion [13]. Montelukast sodium is a potent and selective cysteinyl leukotriene receptor antagonist that is being investigated in the treatment of asthma [14-15]. In present work, we have investigated the inhibition action of Montelukast sodium as corrosion inhibitor of mild steel (MS) in 1 M HCl using weight loss, electrochemical and quantum chemical methods.

## 2. EXPERIMENTAL

### 2.1. Metal samples and Inhibitor

The experiments were performed on mild steel (MS) having the composition (wt. %): 0.076% C, 0.192% Mn, 0.012% P, 0.026% Si, 0.050% Cr, 0.023% Al, 0.123% Cu and balance Fe. Mild steel strips with dimensions of 2.5 cm  $\times$  2 cm  $\times$  0.025 cm were used for the weight loss studies. The electrode (mild steel) having 8 cm  $\times$  1 cm  $\times$  0.025 cm sizes with an exposed area of 1 cm<sup>2</sup> and rest being covered by epoxy resin was used as working electrode for electrochemical study.

Montelukast Sodium tablets were commercially obtained as a trade name Montek-10 manufactured by the Sun Pharma Sikkim. The compound is in its purest state, having molecular formula (C<sub>35</sub>H<sub>35</sub>ClNNaO<sub>3</sub>S) and molecular weight (608.18). Its chemical structure is shown in Figure1.

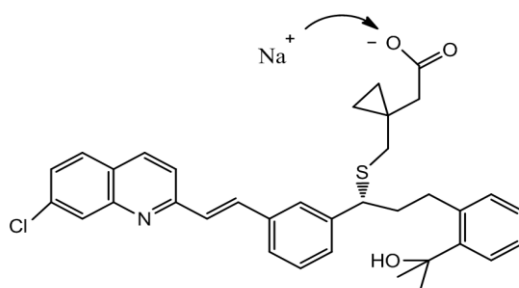


**Figure1.** Molecular structure of 2-[1-[[1-[3-[2-[(7-Chloro-2-quinoly)] vinyl] phenyl]-3-[2-(1-hydroxy-1-methyl-ethyl)phenyl]-propyl]sulfanylmethyl]cyclopropyl]acetic acid sodium salt.

### 2.2. Quantum chemical calculations

Theoretical calculations were carried out using density function theory (DFT) method, B3LYP with electron basis set 6-31G\* (d, p) for all atoms. Calculations were executed with Gaussian 03, E

.01. Quantum chemical parameters such as energy of highest occupied molecular orbital ( $E_{\text{HOMO}}$ ), lowest unoccupied molecular orbital ( $E_{\text{LUMO}}$ ), total energy ( $\Delta E_{\text{LUMO-HOMO}}$ ), and dipole moment ( $\mu$ ) were determined [16].

### 2.3. Gravimetric measurement

The MS specimens having dimensions (2.5 cm  $\times$  2.0 cm  $\times$  0.025 cm) were abraded with series of emery paper (600-1200 grades) washed with distilled water and finally with acetone. The mild steel specimens were dipped into conical flasks which contained 100 mL of 1 M HCl in the absence and presence of different concentration of inhibitor. The conical flask having test solutions were kept in thermostat. After 3 h, the specimens were taken out, washed, dried and weighed accurately. The mean corrosion rate as expressed in  $\text{mg cm}^{-2}$  with respect to acid and inhibitor was calculated. The tests were repeated with optimum concentration at different temperatures. The corrosion rate ( $C_{\text{R}}$ ) was calculated from the following equation,

$$C_{\text{R}} (\text{mm/y}) = \frac{87.6W}{atD} \quad (1)$$

where  $W$  is the average weight loss of MS specimens,  $a$  total area of MS specimen,  $t$  is the immersion time (3 h) and  $D$  is density of MS in ( $\text{gcm}^{-3}$ ). The inhibition efficiency ( $\eta\%$ ) of the inhibitor was calculated as follows;

$$\eta\% = \frac{C_{\text{R}} - {}^{\text{inh}}C_{\text{R}}}{C_{\text{R}}} \times 100 \quad (2)$$

where  $C_{\text{R}}$  and  ${}^{\text{inh}}C_{\text{R}}$  are the corrosion rates of MS in the absence and presence of the inhibitors, respectively

### 2.4. Electrochemical measurements

The corrosion behavior of mild steel in the presence and absence of inhibitor in 1 M HCl were used to study by electrochemical method. Experiments were performed in conventional three electrode cell. Three electrodes connected to Potentiostat/Galvanostat G300-45050 (Gamry Instruments Inc., USA). Echem Analyst 5.0 software package was used for data fitting. Mild steel strip act as working electrode, platinum electrode was used as an auxiliary electrode and standard calomel electrode (SCE) as reference electrode. Tafel curves were obtained by changing the electrode potential automatically from  $-0.25$  V to  $+0.25$  V versus open corrosion potential at a scan rate of  $1.0 \text{ mVs}^{-1}$ . Linear Polarization Resistance (LPR) experiments were done from  $-0.02$  V to  $+0.02$  V versus corrosion potential at the scan rate of  $0.125 \text{ mVs}^{-1}$ . EIS measurements were performed under potentiostatic conditions in a frequency range from 100 kHz to 0.01 Hz, with amplitude of 10mV AC signal.

### 3. RESULTS AND DISCUSSION

#### 3.1. Electrochemical measurements

##### 3.1.1. Potentiodynamic polarization measurements

Potentiodynamic polarization curves of mild steel in 1 M HCl in the presence and absence of Montelukast sodium are shown in Figure 2. As the concentration of inhibitor increases, there is decrease in  $I_{\text{corr}}$  values due to decrease in the corrosion rate[17]. Corrosion potential ( $E_{\text{corr}}$ ), corrosion current density ( $I_{\text{corr}}$ ), anodic and cathodic slopes ( $\beta_a$  and  $\beta_c$ ) obtained from the Tafel plots are given in Table 1. The inhibition efficiencies were calculated from  $I_{\text{corr}}$  values obtained using following equation;

$$\eta\% = \frac{I_{\text{corr}} - I_{\text{corr(inh)}}}{I_{\text{corr}}} \times 100 \quad (3)$$

where  $I_{\text{corr}}$  and  $I_{\text{corr(inh)}}$  are the corrosion current density of MS in 1 M HCl in the absence and presence of inhibitor.

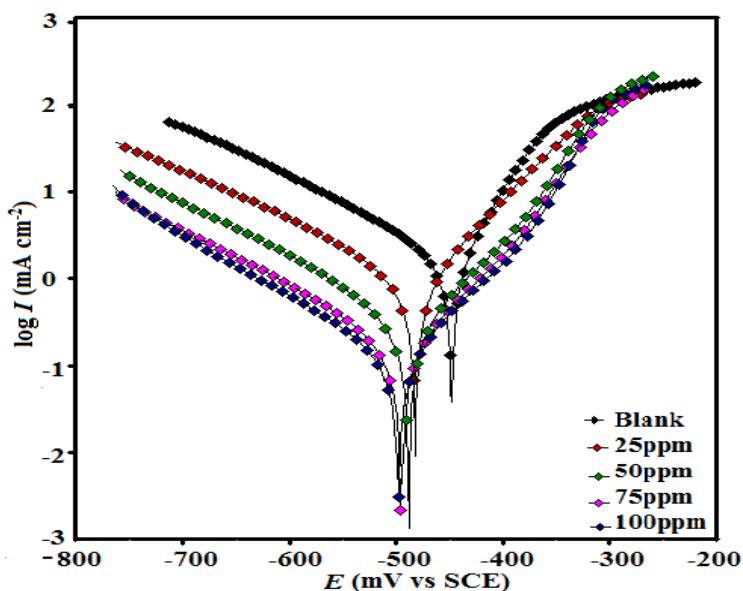


**Figure 2.** Polarisation curves of mild steel in 1 M HCl in the presence and absence of Montelukast sodium.

The anodic and cathodic slopes ( $\beta_a$  and  $\beta_c$ ) values obtained from the Tafel plots remains more or less identical indicating that the effect of inhibitors does not change the mechanism of corrosion [18]. The corrosion potential values above 85 mV in inhibited solution with respect to uninhibited solution, results in cathodic or anodic inhibitor [19]. The result obtained for Montelukast sodium as inhibitor shows values between 27- 44 mV of corrosion potential ( $E_{\text{corr}}$ ), which suggests that it is a

mixed type inhibitor [20-21]. The values of corrosion current densities ( $I_{corr}$ ) and polarization resistance ( $R_p$ ) are given in Table 1.

**Table 1.** Polarization data for MS in 1 M HCl in absence and presence of different concentration of Montelukast sodium

Inhibitor concentration(ppm)	Tafel Polarization			Linear Polarization			
	$E_{corr}$ (mVvs SCE)	$\beta_a$ (mV/dec)	$\beta_c$ (mV/dec)	$I_{corr}$ ( $\mu A cm^2$ )	$\eta\%$	$R_p$ ( $\Omega cm^2$ )	$\eta\%$
Blank	-448	46	96	1070	-	14.0	-
25	-475	88	161	700	34.5	23.6	40.8
50	-483	101	147	336	68.5	75.6	81.4
75	-489	107	207	179	83.2	147.2	90.4
100	-492	54	70	70	93.3	185.6	92.4

3.1.2. Electrochemical impedance spectroscopy (EIS)

Figure 3 shows the Nyquist plots and Equivalent circuit for mild steel in 1 M HCl solution in the absence and presence of inhibitor at various concentrations. The corresponding Bode and phase angle plots are shown in Figure 4.

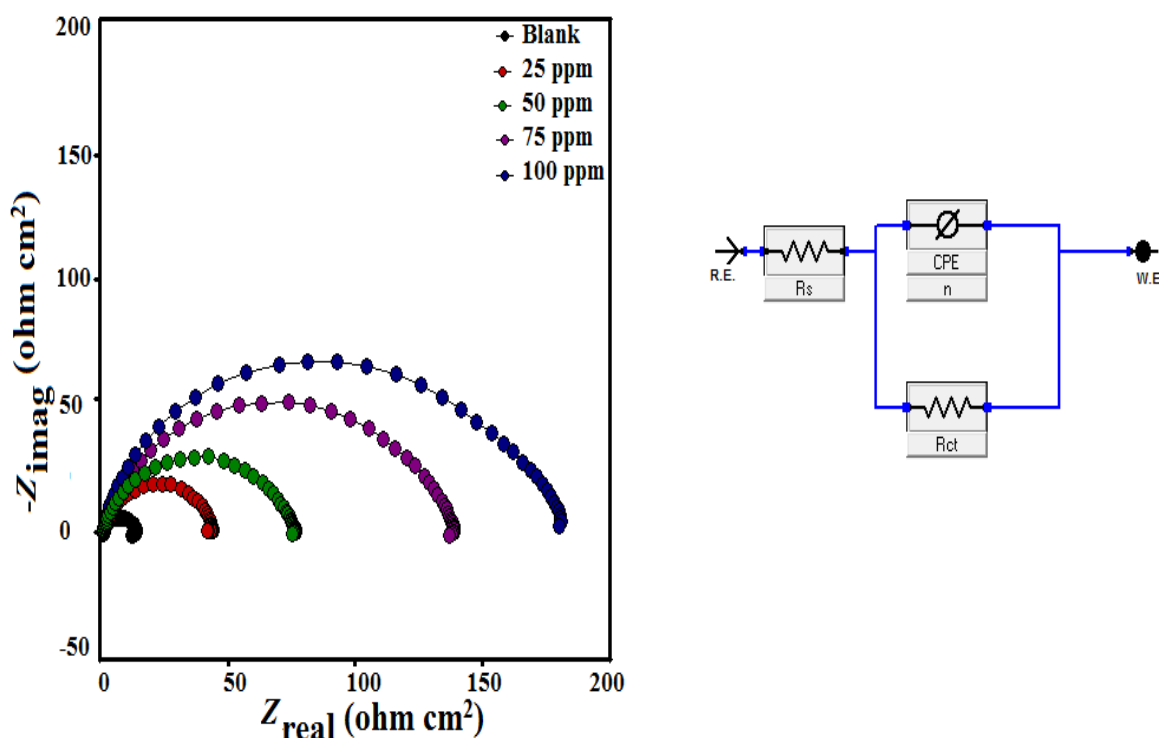


**Figure 3.** Nyquist plot and Equivalent circuit for MS in 1M HCl in the presence and absence of different concentrations of Montelukast sodium

**Table 2.** Electrochemical impedance parameters and corresponding efficiencies of MS in 1 M HCl at different concentration of Montelukast sodium

Inhibitor concentration(ppm)	$R_{ct}$ ( $\Omega \text{ cm}^2$ )	$n$	$Y_0$ ( $10^{-6}\Omega^{-1} \text{ cm}^{-2}$ )	$C_{dl}$ ( $\mu\text{F cm}^{-2}$ )	$\eta\%$
Blank	12.1	0.868	242.6	100.6	-
25	39.8	0.882	111.0	56.3	69.6
50	74.9	0.861	93.46	43.5	83.7
75	133.3	0.855	61.57	28.6	90.9
100	173.2	0.855	45	23.8	93.0

The Nyquist plots are regarded as semicircles. Nyquist plots can be modelled by a simple circuit including the charge transfer resistance ( $R_{ct}$ ) parallel with double layer capacitance ( $C_{dl}$ ) in series with solution resistance ( $R_s$ ) [22].

$$C_{dl} = Y_0 (\omega_{max})^{n-1} \quad (4)$$

Where  $Y_0$  is CPE coefficient,  $n$  is CPE exponent (phase shift),  $\omega$  is the angular frequency. All the data obtained are listed in (Table 2).

In case of electrochemical impedance spectroscopy, the inhibition efficiency was calculated using charge transfer resistance ( $R_{ct}$ ) as follows;

$$\eta\% = \frac{R_{ct(inh)} - R_{ct}}{R_{ct(inh)}} \times 100 \quad (5)$$

where  $R_{ct(inh)}$  and  $R_{ct}$  are the values of charge transfer resistance in the presence and absence of inhibitor in 1 M HCl respectively. As inhibitor concentration increases the charge transfer resistance increases and double layer charging capacitance decreases in 1 M HCl. Decrease in the capacitance may be attributed to a decrease in local dielectric and increase in the thickness of electrical double layer [23].

$$C_{dl} = \frac{\epsilon\epsilon_0 A}{d} \quad (6)$$

where  $\epsilon_0$  is the vacuum dielectric constant,  $\epsilon$  is the local dielectric constant,  $d$  is the thickness of the double layer, and  $A$  is the surface area of the electrode. Decrease in  $C_{dl}$  depends upon adsorption of inhibitor molecules; capacitance is inversely proportional to the thickness of the double layer [24].

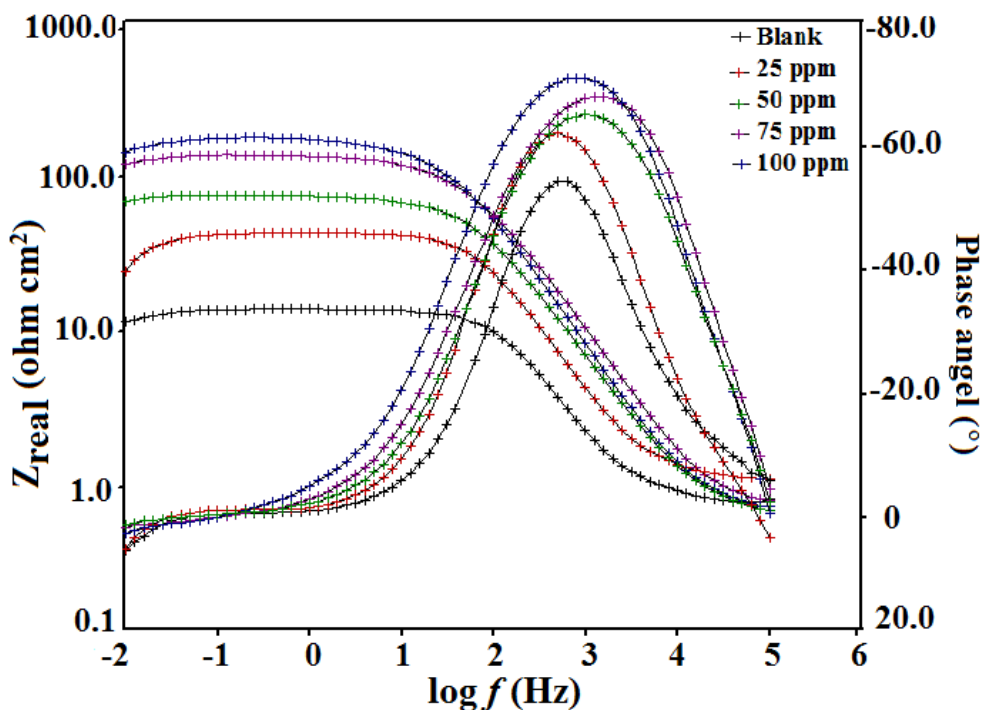


**Figure 4.** Bode-impedance and Phase angle plots for MS in 1 M HCL and different concentration of Montelukast sodium

3.2. Weight loss measurements

The correlation of inhibition efficiency at different conditions is shown in Figure 5. Efficiency increases with increasing inhibitor concentration at a certain point i.e optimum concentration (97% at 100 ppm) after that it remained constant. The efficiency of Montelukast sodium decreases with increasing time due increase in corrosion rate. Increase in temperature causes increase in corrosion of metal due to increase in evolution of H<sub>2</sub> gas [25]. The weight loss results obtained for MS in 1 M HCl in the presence and absence of the different concentration of inhibitor are summarized in Table 3.

**Table 3.** Weight loss measurements for MS in 1 M HCl at different concentrations of the inhibitor

Inhibitor concentration(ppm)	Weight loss (mg cm <sup>-2</sup> )	$\eta\%$	$C_R$ (mm/y)	$\theta$
Blank	20.0	-	74.2	-
25	8.5	57.5	31.5	0.57
50	5.9	70.5	21.8	0.70
75	2.8	86.0	10.3	0.86
100	0.6	97.1	2.2	0.97

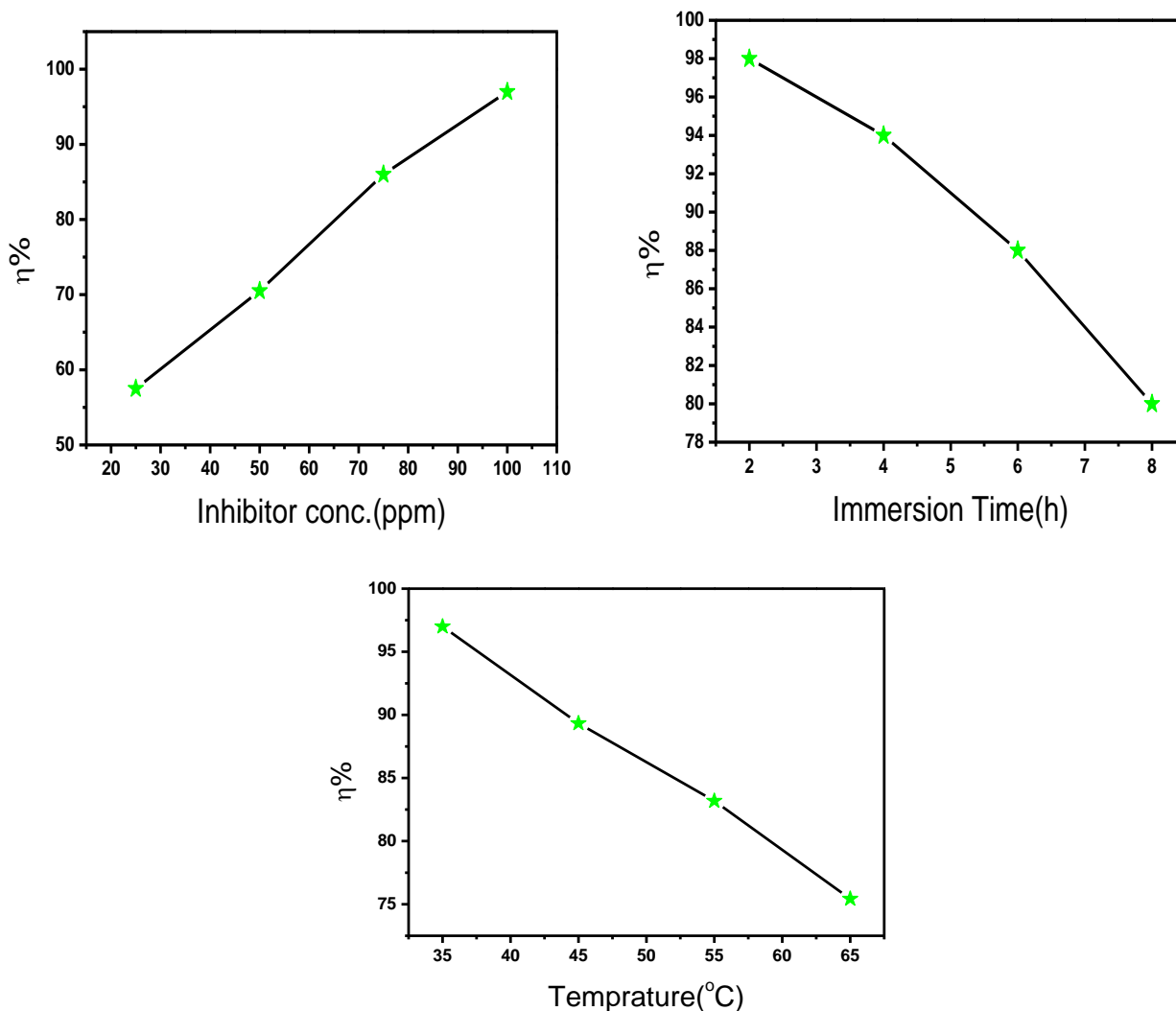


**Figure 5.** The correlation of efficiency at (a) different concentrations (b) Temperatures and (c) Immersion time.

### 3.2.1. Adsorption isotherm

The interaction between the inhibitor and mild steel surface can be elaborate using adsorption isotherms. The surface coverage ( $\theta$ ) was calculated according to the following equation,

$$\theta = \frac{w_0 - w_i}{w_0} \tag{7}$$

where  $w_0$  and  $w_i$  are the values of the corrosion weight losses of mild steel in the absence and presence of inhibitors, respectively. The plot of  $(C/\theta)$  vs  $(\theta)$  yields straight line with nearly unit slope and the best fits are obtained with Langmuir adsorption isotherm as presented in Figure 6. The linear correlation coefficient ( $R^2 = 0.9992$ ) is much closed to 1.0 clearly proving that the adsorption of inhibitor on the mild steel surface obeys the Langmuir adsorption isotherm [26].

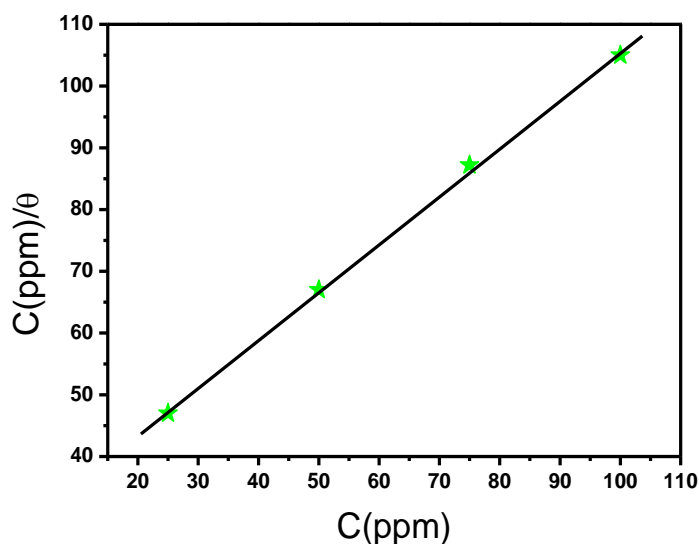


**Figure 6.**The Langmuir adsorption isotherm plots for MS in 1 M HCl with Montelukast sodium.

3.2.2. Thermodynamic activation parameters

The mechanism of inhibition can be understood from the data obtained from the thermodynamic parameters. A plot of the corrosion rate,  $\ln C_R$  vs  $1000/T$  gave straight line as shown in Figure 7(a). The apparent activation energy ( $E_a$ ) was calculated by using following equation;

$$\ln(C_R) = \frac{-E_a}{RT} + A \tag{8}$$

where  $E_a$  is activation energy for the corrosion of MS in 1 M HCl,  $R$  is the gas constant,  $A$  the Arrhenius pre-exponential factor and  $T$  is the absolute temperature. The values of  $E_a$  in 1 M HCl in the absence and presence of inhibitor were determined from the slope by plotting the values obtained given in Table 4. The increase in activation energy causes decrease in adsorption of the inhibitor on the mild steel surface. The corrosion rate of mild steel increases due to desorption of inhibitor molecules with increasing temperature and surface area of mild steel comes in contact with aggressive environment [27].

$\Delta H^*$  (enthalpy of activation) and  $\Delta S^*$  (entropy of activation) were calculated using the equation;

$$C_R = \frac{RT}{Nh} \exp\left(\frac{\Delta S^*}{R}\right) \exp\left(-\frac{\Delta H^*}{RT}\right) \tag{9}$$

Where  $h$  is Plank constant,  $N$  is Avogadro’s number. Figure 7(b) shows a plot of  $\ln (C_R / T)$  against  $1000/T$  which give straight lines with a slope of  $(-\Delta H^*/R)$  and an intercept of  $[(\ln(R/Nh)) +$

( $\Delta S^*/R$ )] from which the values of  $\Delta H^*$  and  $\Delta S^*$  were calculated and are given in Table 4. The endothermic nature of dissolution of steel is depicted by positive values of enthalpy. The values of  $\Delta S^*$  higher in the presence of inhibitor reveals that randomness increases due to movement of reactants to activated complex [28].

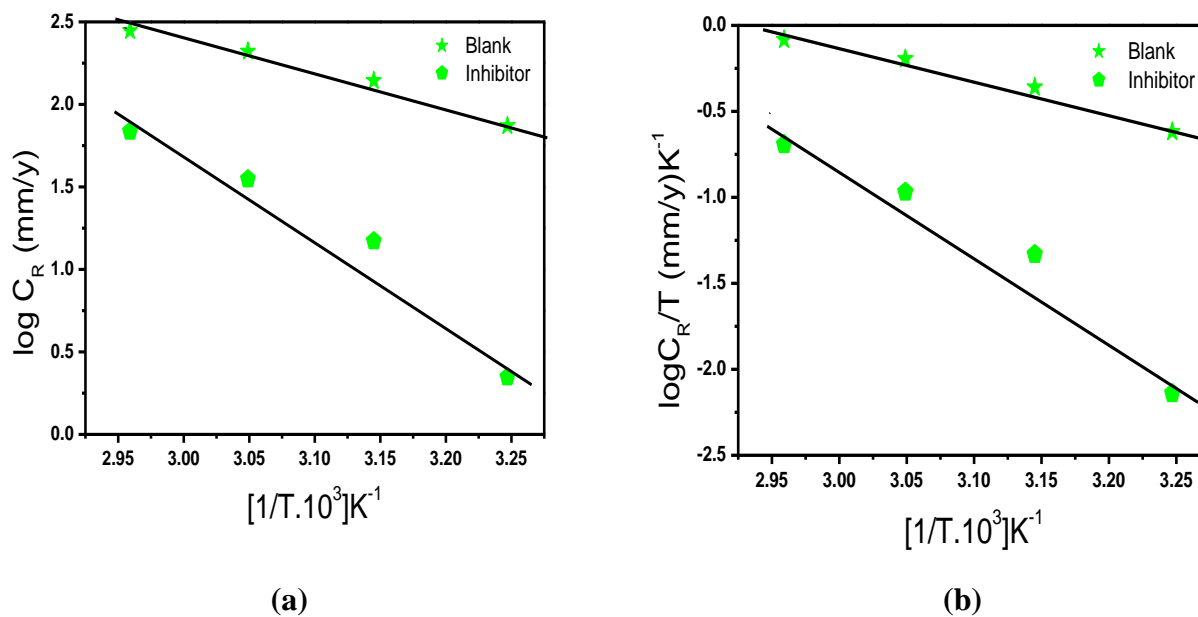


**Figure 7.** Adsorption isotherm plots (a)  $\log C_R$  vs.  $1000/T$  (b)  $\log C_R/T$  vs.  $1000/T$  for MS in 1M HCl in the absence and the presence inhibitor

**Table 4.** Thermodynamic parameters for mild steel in 1 M HCl in absence and presence of Montelukast sodium

Inhibitor concentration(ppm)	$E_a$ (kJmol <sup>-1</sup> )	$\Delta H^*$ (kJmol <sup>-1</sup> )	$\Delta S^*$ (Jmol <sup>-1</sup> K <sup>-1</sup> )
Blank	38.15	35.47	-93.62
100	97.18	94.50	70.78

The standard free energy of adsorption  $\Delta G_{ads}$  and the values of equilibrium constant  $K_{ads}$  at different temperatures were calculated from the equation;

$$K_{ads} = \frac{\theta}{C(1-\theta)} \tag{10}$$

The equation can be rearranged as;

$$\frac{C}{\theta} = \frac{1}{K_{\text{ads}}} + C \quad (11)$$

Where C is concentration of inhibitor and  $\theta$  is surface area.

$$\Delta G_{\text{ads}} = -RT \ln(55.5K_{\text{ads}}) \quad (12)$$

The value 55.5 in the above equation is the concentration of water in solution in mol/lit. The values of  $\Delta G_{\text{ads}}$  are given in Table 5 [29-30].

**Table 5.** Standard free energy of adsorption of mild steel in 1 M HCl in the absence and presence of inhibitor at different temperatures

Temperature(°C)	$-\Delta G_{\text{ads}}$ (kJ mol <sup>-1</sup> )
35	41.50
45	39.28
55	39.0
65	38.93

The calculated values of  $\Delta G_{\text{ads}}$  are in range from -41.50 to -38.93 KJ mol<sup>-1</sup> indicating that the adsorption of the inhibitor molecule on MS surface may involve chemical adsorption [31].

### 3.3. Quantum Chemical Calculations

Quantum chemical parameters for Montelukast sodium such as  $E_{\text{HOMO}}$  (high occupied molecular orbital energy),  $E_{\text{LUMO}}$  (lowest unoccupied molecular orbital energy) and the dipole moment ( $\mu$ ) were calculated. The results are given in Table 6.

**Table 6.** Calculated quantum chemical parameters of studied Montelukast sodium drug

Quantum Parameters	Montelukast sodium
$E_{\text{HOMO}}$ (hartree)	-0.08790
$E_{\text{LUMO}}$ (hartree)	-0.15674
$\Delta E_{\text{LUMO-HOMO}}$ (hartree)	-0.06884
Dipole Moment ( $\mu$ )	4.8426

The inhibition efficiency of the inhibitor depends upon energy gap between the  $E_{\text{HOMO}}$  and  $E_{\text{LUMO}}$ ; lower the value of  $\Delta E_{\text{LUMO-HOMO}}$ , the higher the inhibition efficiency [32]. Polarity of a covalent bond (Dipole moment  $\mu$ ) can be understood by distribution of electrons in a molecule and large values of dipole moment  $\mu$  favour the adsorption of inhibitor. The vacant 3d orbital of Fe atom

attaches with the HOMO of the inhibitors;  $E_{\text{HOMO}}$  has tendency to donate electron whereas the filled 4s orbital attach to LUMO of the inhibitors,  $E_{\text{LUMO}}$  has tendency to accept electron. The interaction between 3d, 4s orbital of Fe atoms and frontier molecular orbital is the deciding factor for adsorption of inhibitor on metal surface [33]. The optimized molecular structures and frontier molecular orbital density distribution of Montelukast sodium are shown in Figure 8. In our earlier work, we investigated Cetirizine as a corrosion inhibitor and if we compare  $\Delta E_{\text{LUMO-HOMO}}$  of both the inhibitors, Montelukast sodium inhibits more than Cetirizine [34].

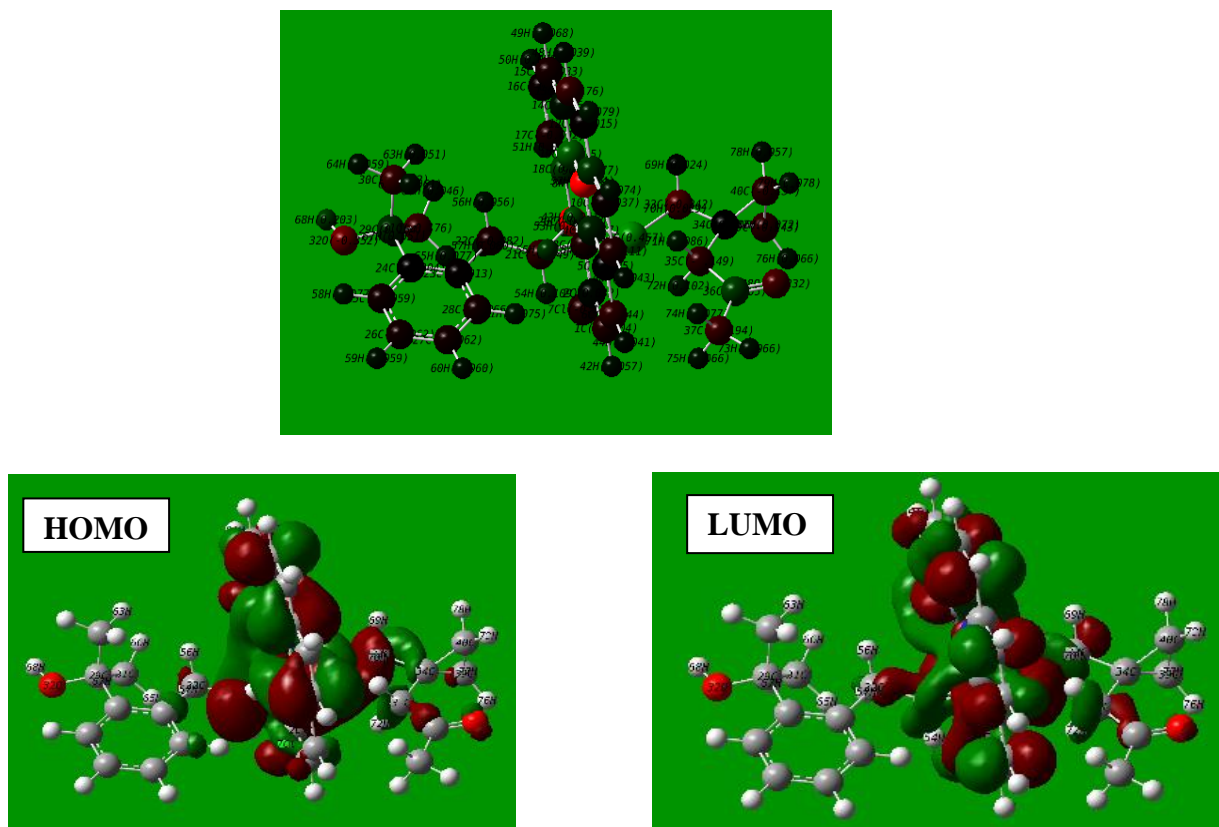


**Figure 8.** Optimized molecular structure and frontier molecular orbital density distribution of Montelukast sodium drug.

#### 3.4. Surface characterization by Optical microanalysis

The mild steel surface before and after immersion in test solutions was studied by optical microscopy [35]. Optical microscopy pictures in Figure 10 reveal the effect on mild steel surface. In Figure 10(a) the picture depicts the normal mild steel specimen after grading with emery paper. Figure 10(b) and (c) shows the condition of metal after dipping it in test solution. The metal surface in contact with inhibitor is in better condition than the one dipped in acid solution. The metal surface is protected due to adsorption of Montelukast sodium on metal surface [36]. This indicated that the inhibitor molecules hinder the dissolution of iron by forming protective film on mild steel surface and thereby reducing the corrosion rate.

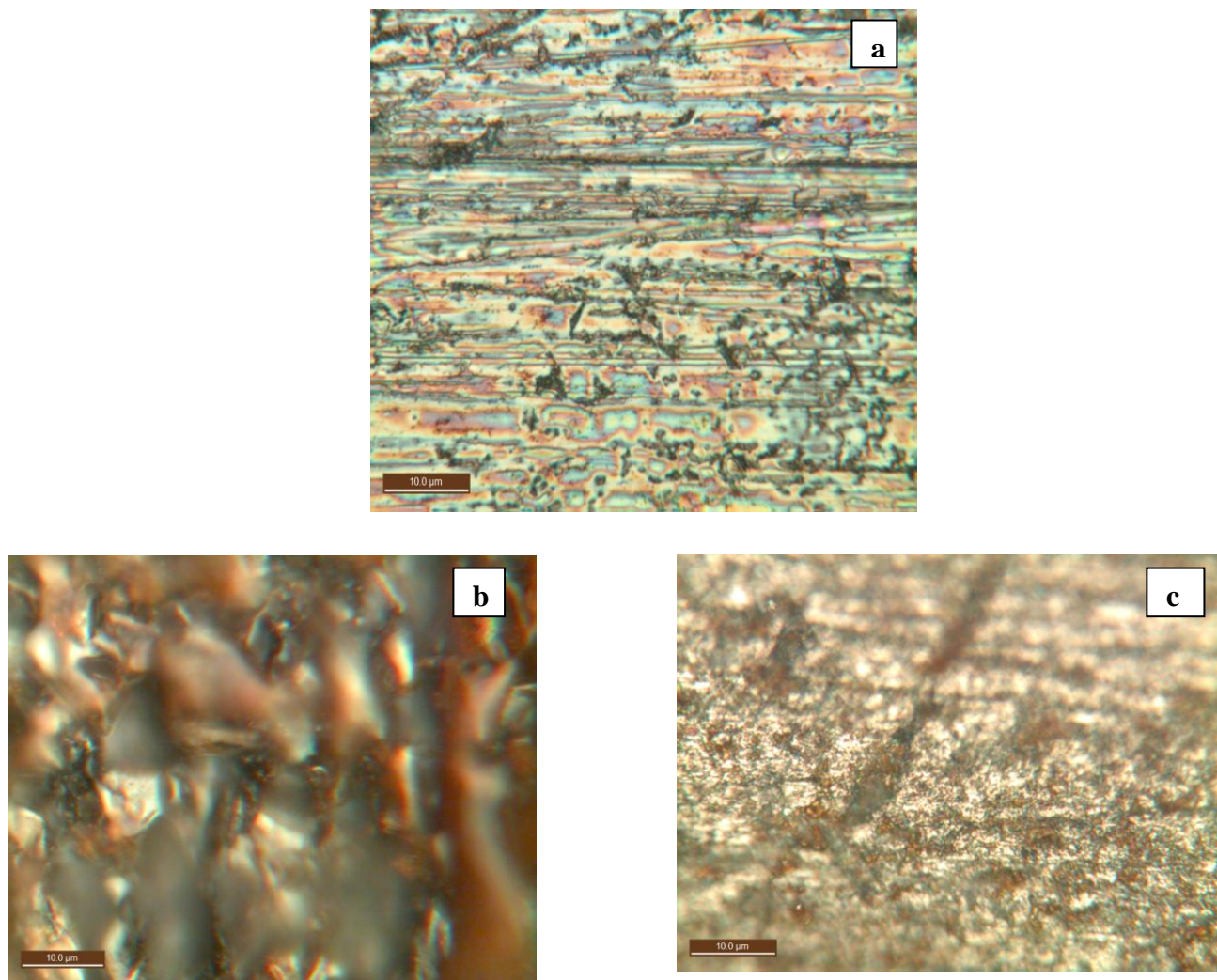
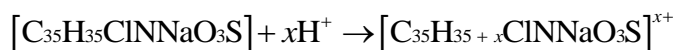


**Figure 10.** Optical microscopy of mild steel surface (a) Polished mild steel, (b) Mild Steel in HCl, (c) Inhibited mild steel sample

### 3.5. Mechanism of adsorption and inhibition

Montelukast sodium prevents corrosion by controlling both the anodic and cathodic reactions. In acidic solutions, Montelukast sodium exists as protonated species.



The adsorption of Montelukast sodium on metal surface can be elucidated by the following ways- (i) Protonated species adsorb on the cathodic sites of the mild steel and decrease the evolution of hydrogen (electrostatic attraction). The adsorption on anodic sites occurs through (ii)  $\pi$ -electron of aromatic ring and (iii) lone pair of electrons of hetero atom which decreases anodic dissolution of mild steel [37]. Thus, formation of protective film on mild steel surface took place which retard metal dissolution.

#### 4. CONCLUSIONS

- (a) Montelukast sodium is a good inhibitor (97% inhibition efficiency observed at 100 ppm) for MS in 1 M HCl.
- (b) Polarization curves indicated that Montelukast sodium is a mixed-type inhibitor. The inhibition efficiencies obtained from polarization and EIS were in good agreement.
- (c) The adsorption of inhibitor molecules on the MS surface in 1 M HCl solution followed Langmuir adsorption isotherm.
- (d) The values obtained for  $\Delta G_{\text{ads}}$  showed chemisorption.
- (e) Quantum chemical method provided good approach of adsorption depicted by  $\Delta E_{\text{LUMO-HOMO}}$  of Montelukast sodium.
- (f) Optical microscopy clearly revealed the surface of MS in test solutions.

#### ACKNOWLEDGEMENT

Priyanka Singh is thankful to UGC New Delhi for the Project (40-101/2011) SR, Fellowship.

#### References

1. Z. Tao, S. Zhang, W. Li, B. Hou, *Corros. Sci.* 51 (2009) 2588
2. M.M. Solomon, S.A. Umoren, I.I. Udoso, A.P. Udoh, *Corros. Sci.* 52 (2010) 1317
3. H. Ashassi-Sorkhabi, S.A. Nabavi-Amri, *Electrochim. Acta* 47 (2002) 2239
4. H. Ashassi-Sorkhabi, B. Shaabani, D. Seifzadeh, *Electrochim. Acta* 50 (2005) 3446
5. I. Ahamad, M.A. Quraishi, *Corros. Sci.* 52 (2010) 651
6. G. Gece, *Corros. Sci.* 53 (2011) 3873
7. S.E. Nataraja, T.V. Venkatesha, H.C. Tandon, B.S. Shylesha, *Corros. Sci.* 53(2011) 4109
8. M.S. Morad, *Corros. Sci.* 50 (2008) 436
9. I.B. Obot, N.O. Obi-Egbedi, *Corros. Sci.* 52 (2010) 198
10. P. Xuehui, R. Xiangbin, K. Fei, X. Jiandong, H. Baorong, *Chinese J. Chem. Eng.* 18 (2010) 337
11. M.M. El-Naggar, *Corros. Sci.* 49 (2007) 2226
12. M. Abdallah, *Corros. Sci.* 44 (2002) 717
13. M. Lebrini, F. Bentiss, H. Vezin, M. Lagrene'e, *Corros. Sci.* 48 (2006) 1279
14. H. Ochiai, N. Uchiyama, T. Takano, K. Hara, T. Kamei, *J. Chromatogr.* 713 (1998) 409
15. M. Saravanan, K. S. kumari, P. P. Reddy, M.N. Naidu, J. M. Babu, A. K. Srivastava, T. L. Kumar, B.V.V.N. Chandra Sekhar, B. Satyanarayana, *J. Pharm. Biomed. Anal.* 48, (2008) 708
16. Gaussian 03, Revision E.01, M.J. Frisch, G.W. Trucks, H.B. Schlegel, G.E. Scuseria, M.A. Robb, J.R. Cheeseman, Jr. J.A. Montgomery, T. Vreven, K.N. Kudin, J.C. Burant, J.M. Millam, S.S. Iyengar, J. Tomasi, V. Barone, B. Mennucci, M. Cossi, G. Scalmani, N. Rega, G.A. Petersson, H. Nakatsuji, M. Hada, M. Ehara, K. Toyota, R. Fukuda, J. Hasegawa, M. Ishida, T. Nakajima, Y. Honda, O. Kitao, H. Nakai, M. Klene, X. Li, J.E. Knox, H.P. Hratchian, J.B. Cross, V. Bakken, C. Adamo, J. Jaramillo, R. Gomperts, R.E. Stratman, O. Yazyev, A.J. Austin, R. Cammi, C. Pomelli, J.W. Ochterski, P.Y. Ayala, K. Morokuma, G.A. Voth, P. Salvador, J.J. Dannenberg, V.G. Zakrzewski, S. Dapprich, A.D. Daniels, M.C. Strain, O. Farkas, D.K. Malick, A.D. Rabuck, K. Raghavachari, J.B. Foresman, J.V. Ortiz, Q. Cui, A.G. Baboul, S. Clifford, J. Cioslowski, B.B. Stefanov, G. Liu, Liashenko, A. P. Piskorz, I. Komaromi, R.L. Martin, D.J. Fox, T. Keith, M.A. Al-Laham, C.Y. Peng, A. Nanayakkara, M. Challacombe, P.M.W. Gill, B. Johnson, W. Chen, M.W.

- Wong, C. Gonzalez, J.A. Pople, Gaussian, Inc., Wallingford CT, (2007)
17. X. Li, S. Deng, H. Fu, *Corros. Sci.* 53 (2011) 3241
  18. I. Ahamad, R. Prasad, M.A. Quraishi, *Corros. Sci.* 52 (2010) 3033
  19. E.S. Ferreira, C. Giacomelli, F.C. Giacomelli, A. Spinelli, *Mater. Chem. Phys.* 83 (2004) 129
  20. M.G. Hosseini, M. Ehteshamzadeh, T. Shahrabi, *Electrochim. Acta* 52 (2007) 3680
  21. G. Gunasekaran, L.R. Chauhan, *Electrochim. Acta* 49 (2004) 4387
  22. H. Ashassi-Sorkhabi, D. Seifzadeh, M.G. Hosseini, *Corros. Sci.* 50 (2008) 3363
  23. P. Lowmunkhong, D. Ungthararak, P. Sutthivaiyakit, *Corros. Sci.* 52 (2010) 30
  24. I. Ahamad, R. Prasad, M. A. Quraishi, *J Solid State Electrochem.* 14 (2010) 2095
  25. D.K. Yadav, B. Maiti, M.A. Quraishi, *Corros. Sci.* 52 (2010) 3586
  26. F. Bentiss, C. Jama, B. Mernari, H.E. Attari, L.E. Kadi, M. Lebrini, M. Traisnel, M. Lagrenee, *Corros. Sci.* 51 (2009) 1628
  27. I. Ahamad, R. Prasad, M.A. Quraishi, *Corros. Sci.* 52 (2010) 933
  28. I. Ahamad, M.A. Quraishi, *Corros. Sci.* 51 (2009) 2006
  29. S.K. Shukla, M.A. Quraishi, *Corros. Sci.* 51 (2009) 1007
  30. J. Aljourani, K. Raessi, M.A. Golozar, *Corros. Sci.* 51 (2009) 1836
  31. F. Bentiss, M. Lebrini, M. Lagren'ee, M. Traisnel, A. Elfarouk, H. Vezin, *Electrochim. Acta* 52 (2007) 6865
  32. A.Y. Musa, R.T.T. Jalgham, A.B. Mohamad, *Corros. Sci.* 56 (2012) 176
  33. P. Xuehui, H. Baorong, L. Weihua, L. Faqian, Y.U. Zhigang, *Chin. J. Chem. Eng.* 15(2007) 909
  34. P. Singh, A. Singh, M.A. Quraishi, E.E. Ebenso, *Int. J. Electrochem. Sci.* 7 (2012) xx-yy
  35. D.K. Kima, S. Muralidharan, T.H. Haa, J.H. Baea, Y.C. Haa, H.G. Lee, J.D. Scantlebury, *Electrochim. Acta* 51 (2006) 5259
  36. H. Ashassi-Sorkhabi, S.A. Nabavi-Amri, *Electrochim. Acta* 47 (2002) 2239
  37. S. K. Shukla, M. A. Quraishi, E. E. Ebenso, *Int. J. Electrochem. Sci.* 6 (2011) 2912